J. Biochem. 126, 313-319 (1999)

Stimulation of Peroxidase Activity by Decamerization Related to Ionic Strength: AhpC Protein from *Amphibacillus xylanus*[1]

Ken Kitano,* Youichi Niimura,† Yoshitaka Nishiyama,† and Kunio Miki*,[2]

*Department of Chemistry, Graduate School of Science, Kyoto University, Sakyo-ku, Kyoto 606-8502; and †Department of Bioscience, Tokyo University of Agriculture, Setagaya-ku, Tokyo 156-8502

Received April 21, 1999; accepted May 25, 1999

AhpC protein, purified from *Amphibacillus xylanus* with a molecular mass of 20.8 kDa, protects cells against oxidation damage. The enzyme catalyses the reduction of hydroperoxides in cooperation with the 55 kDa flavoprotein, *A. xylanus* NADH oxidase (NADH oxidase-AhpC system). *A. xylanus* AhpC has two disulfide linkages between monomers and can act in the homodimer form. Gel-filtration column chromatography and dynamic light scattering (DLS) suggest that *A. xylanus* AhpC also forms a large oligomeric assembly (10-12 mers). *A. xylanus* AhpC was crystallized and X-ray diffraction data were collected to 3.0 Å. The self-rotation function revealed fivefold and twofold axes located perpendicularly to each other, suggesting that the molecular assembly of *A. xylanus* AhpC is composed of ten monomers. The oligomerization of *A. xylanus* AhpC is affected by ionic strength in the DLS measurements. The H_2O_2 reductase activity of the *A. xylanus* NADH oxidase-AhpC system is also affected by ionic strength, and it was found that the decamerization of AhpC might be required for the activation of the NADH oxidase-AhpC system.

Key words: AhpC, decamer, dynamic light scattering, ionic strength, peroxidase activity.

Reactive oxygen species such as $O_2^{\cdot-}$ and H_2O_2, which are mainly produced by the incomplete reduction of oxygen during respiration, damage cellular components including DNAs and proteins (*1*). Organisms living in an aerobic environment have developed defense systems involving various antioxidant enzymes against such oxidative stress. AhpC protein (*2*), also called thiol-specific antioxidant protein (TSA) or peroxiredoxin (Prx), represents a family of newly discovered peroxidases (*3*). These proteins, with molecular masses of 20-25 kDa, are highly conserved in eukaryotes and prokaryotes, and show no sequence homology to previously known antioxidant proteins such as catalases, glutathione peroxidases or superoxide dismutases. All AhpC proteins contain one conserved cysteine in the N-terminal region, which is the site of oxidation by H_2O_2 (*2, 4*). AhpC proteins can be classified into two groups, one containing no other conserved cysteine (1-Cys group) and the other containing an additional conserved cysteine in the C-terminal region (2-Cys group). The oxidized N-terminal cysteine of 2-Cys members rapidly forms an intermolecular disulfide bond with the C-terminal cysteine of another subunit, which is subsequently reduced by electrons supplied by NADH oxidase (*5*), alkyl hydroperoxide reductase (*2*), or thioredoxin (*6*).

Amphibacillus xylanus, isolated from alkaline compost (*7*), has unique phenotypic and chemotaxonomic characteristics as well as unique bioenergetic properties (*8*). *A. xylanus*, which lacks a respiratory system and the heme proteins catalase and peroxidase, has the same growth rate and cell yield under strictly anaerobic and aerobic conditions (*9*). This growth characteristic is due to the presence of anaerobic and aerobic pathways producing similar amounts of ATP (*10*). A 55 kDa flavoprotein, *A. xylanus* NADH oxidase, regenerates NAD^+ from NADH produced in the aerobic pathway. When coupled with *A. xylanus* AhpC (20.8 kDa), NADH oxidase shows extremely high scavenging activity for H_2O_2 (NADH oxidase-AhpC system) compared with other known peroxide scavenging enzymes (Niimura, Y. *et al.*, unpublished results). *A. xylanus* AhpC shows 64.4 and 39.3% homology to *Salmonella typhimurium* (*11-13*) and yeast TSAs (*14*), respectively. These three AhpC (TSA) proteins belong to the 2-Cys group and exist as homodimers formed by intermolecular disulfide linkages. Here we report the characterization of the oligomeric nature of *A. xylanus* AhpC on the basis of preliminary X-ray crystallography, dynamic light scattering (DLS) and turnover activity assays. It was concluded that the oligomerization of *A. xylanus* AhpC is necessary for the activation of the AhpC-NADH oxidase system.

MATERIALS AND METHODS

Preparation of A. xylanus AhpC and NADH Oxidase—*A. xylanus* AhpC and NADH oxidase proteins were overexpressed in *E. coli* and purified according to the established procedures (Niimura, Y. *et al.*, unpublished results). The proteins were judged to be highly homogeneous by SDS-PAGE. *A. xylanus* AhpC was concentrated to 30 mg/ml in 100 mM HEPES-NaOH buffer (pH 7.5). *A. xylanus* NADH

[1] This work was partly supported by the "Research for the Future" Program of the Japanese Society for the Promotion of Science (JSPS) to K.M. (JSPS-RFTF 97L00501). K.K. is supported by a Grant-in-Aid for JSPS Fellows (No. 9605).

[2] To whom correspondence should be addressed. Tel: +81-75-753-4029, Fax: +81-75-753-4032, E-mail: miki@kuchem.kyoto-u.ac.jp

oxidase was concentrated to 10 mg/ml in 50 mM sodium phosphate buffer (pH 7.0) containing 0.5 mM EDTA. Protein samples were filtered and stored at 4°C.

Gel-Filtration Column Chromatography of A. xylanus AhpC—The gel-filtration column chromatography of *A. xylanus* AhpC was performed at room temperature using FPLC (Amersham Pharmacia Biotech). The column (TSK-GEL G3000SW, 7.8×300 mm, TOSOH, Tokyo) was equilibrated with 100 mM HEPES-NaOH buffer (pH 7.5) containing 100 mM sodium sulfate, and 140 μg of purified *A. xylanus* AhpC was applied. The elution of *A. xylanus* AhpC was monitored at 280 nm (Fig. 1).

Dynamic Light Scattering (DLS) of A. xylanus AhpC—Dynamic light scattering (DLS) is a unique technique for measuring the translational diffusion coefficient (D_T) of a macromolecule undergoing Brownian motion in solution. By observing the monochromatic light scattered by moving particles, intensity fluctuations corresponding to particulate motion can be measured. A decay analysis of the autocorrelation function, a measurement of the time-dependence of the intensity fluctuations, of the light scattering signal can afford quantitative information about the hydrodynamic radius (R_H) of macromolecules. At the same time, the sample polydispersity can be judged because this technique is exquisitely sensitive to the oligomeric state of macromolecules, *i.e.*, the intensity of scattered light is proportional to the square of the mass of the solute particle (*15-19*). As monodispersity of the sample solution is generally required for protein crystallization, DLS has become a widely employed method to check the oligomeric state of macromolecular samples, to eliminate the non-monodispersity conditions prior to numerous crystallization trials (*20-26*). DLS measurements were performed using DynaPro-801 operated with the program DYNAMICS (Protein Solution, USA) to estimate the molecular mass of *A. xylanus* AhpC at various ionic strengths. *A. xylanus* AhpC samples (144 μM) in 100 mM HEPES-NaOH buffer (pH 7.5) with various salt concentrations were prepared in 250 μl aliquots and filtered through a 0.02 μm membrane (Whatman Int.). The protein was stable throughout the measurements and no aggregation was observed. Protein samples were loaded into sample cells previously equilibrated with buffer solutions containing salt, and illuminated with a solid-state laser at 25°C. The D_T measurements were repeated 5 times and averaged for each sample. R_H is derived from D_T by the Stokes-Einstein equation (Eq. 1).

$$R_H = kT/6\pi\eta D_T \quad (1)$$

where k, T, and η are the Boltzmann constant, absolute temperature and viscosity, respectively. As R_H is sensitive to the viscosity η of the solution, the influence of salts at each concentration on η was corrected by applying the viscosity of protein-free salt solutions (data not shown). Finally the molecular mass of *A. xylanus* AhpC was calculated from R_H using DYNAMICS, which includes a standard curve for globular proteins (Fig. 2).

Crystallization of A. xylanus AhpC—Crystallization conditions for *A. xylanus* AhpC were screened preliminarily using Crystal Screen and Grid-Screen kits (Hampton Research, Riverside, CA, USA) at 20°C by sitting-drop vapor diffusion (*27*). Needle-shaped crystals were obtained at 25 mg/ml protein, 30% polyethylene glycol (PEG) 6000, and 100 mM ammonium acetate in 100 mM HEPES-NaOH buffer at pH 7.0 (Fig. 3A). Crystals grew to 0.5 mm in length but less than 50 μm in diameter, a size not suitable for X-ray diffraction studies. Further crystallization trials afforded well-shaped *A. xylanus* AhpC crystals of 0.8×0.8×0.8 mm^3 in size after two days growth, under the conditions of 25 mg/ml protein, 26% PEG6000, 100 mM sodium sulfate, and 100 mM ammonium acetate in 100 mM MES-NaOH buffer at pH 5.5 (Fig. 3B). The pH optimization was critical for crystal growth. Many other salts, such as sodium chloride, potassium phosphate, ammonium sulfate, sodium sulfate, *etc.*, were used instead of ammonium acetate as additives for crystallization, but no crystals were obtained.

X-Ray Diffraction Experiments on A. xylanus AhpC—Crystals of *A. xylanus* AhpC were mounted in glass capillaries with a trace amount of the mother liquor. Intensity data of the native crystals were collected at 293 K with synchrotron radiation at the BL-6A and 18B beam lines of the Photon Factory (PF), the High Energy Accelerator Research Organization (KEK), Tsukuba (*28*). The diffraction intensities were recorded on Imaging Plates (Fuji

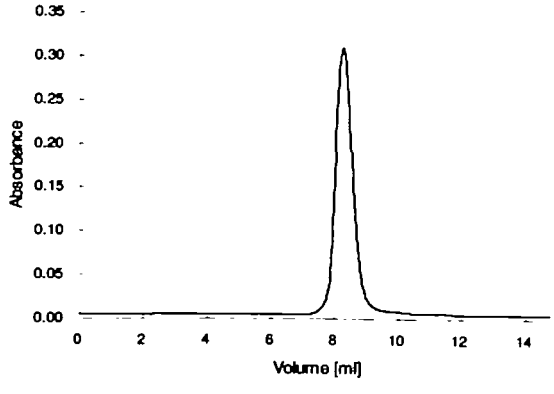

Fig. 1. **Elution pattern from gel-filtration column chromatography of *A. xylanus* AhpC.** Elution was monitored at 280 nm in the presence of 100 mM sodium sulfate.

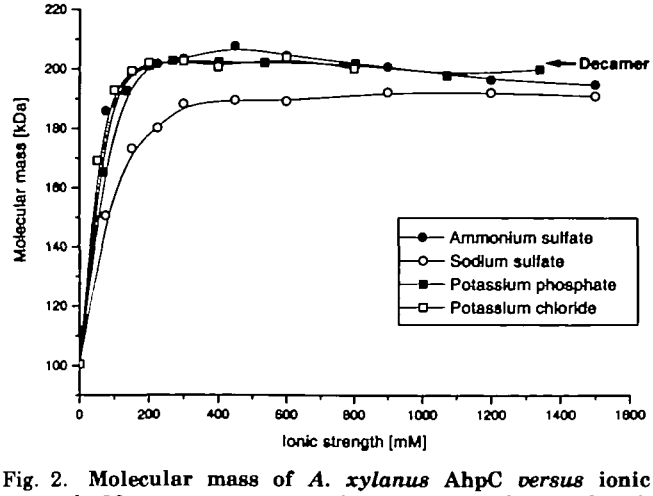

Fig. 2. **Molecular mass of *A. xylanus* AhpC *versus* ionic strength.** Measurements were performed using DLS at 25°C with various salts: ammonium sulfate (○), sodium sulfate (●), potassium phosphate (□), and potassium chloride (■).

Photo Film, Tokyo), which were digitized at 100 μm intervals on a Fujix BAS2000 IP reader (Fig. 4). Data processing was performed using the programs DENZO and SCALEPACK (*29*). Crystal data and data collection statistics are summarized in Table I. The intensity data at 293 K were collected using two crystals with different rotation axes, and these were merged into one data set. The experiments were also performed using frozen crystals placed directly in cold nitrogen streams at 100 K with a trace amount of the mother liquor. In this case, the volume of the unit cell decreased by about 8% compared with crystals at 293 K.

Self-Rotation Function of A. xylanus AhpC—To determine the molecular symmetry of *A. xylanus* AhpC, the self-rotation function (*30*) was calculated using the program PORARRFN (W. Kabsch, 1997) in the CCP4 Program Suite (Collaborative Computational Project, Number 4, 1994) . Orthogonalized axes were chosen according to the Brookhaven format ($x=a$, $y=c^*\times a$ and $z=c^*$). Diffraction data from 15-5.2 Å resolution and a 30 Å integration radius were used for the Patterson map calculation. The $\kappa=180^\circ$

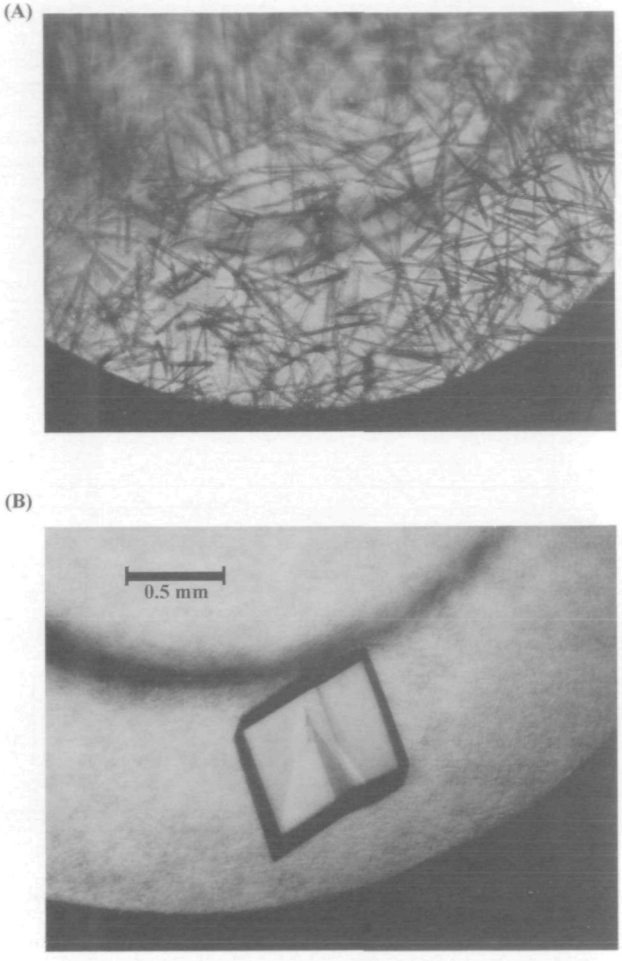

Fig. 3. **Crystals of *A. xylanus* AhpC.** Both A and B show the same scale; the bar indicates 0.5 mm. (A) Preliminary thin, needle-shaped crystals were not suitable for X-ray diffraction experiments. (B) Prismatic crystals of good size and shape were obtained under the optimized crystallization conditions.

TABLE I. **Crystal data and data collection statistics of *A. xylanus* AhpC.**

Crystal data		
Space group	*P*1	
Cell parameters	293 K	100 K
a	79.4 Å	75.5 Å
b	79.2 Å	78.5 Å
c	104.9 Å	103.0 Å
α	77.4°	77.9°
β	82.3°	80.2°
γ	80.0°	82.5°
Data collection statistics at 293 K (collected using two crystals)		
Wave length	1.00 Å	
Camera distance	430 mm	
Resolution limit	3.00 Å	
Number of reflections	118,407 ($I/\sigma>1.0$)	
Number of unique reflections	43,857 ($I/\sigma>1.0$)	
Completeness	89.6% (100-3.00 Å)	
	99.7% (15.0-5.20 Å)	
	67.1% (3.11-3.00 Å)	
$\langle I/\sigma\rangle$	12.3	
R_{merge}	10.4% (100-3.00 Å)	
	7.5% (15.0-5.20 Å)	
	32.4% (3.11-3.00 Å)	

*R_{merge} (%) $=\Sigma(\Sigma_i|I_i-\langle I\rangle|)/\Sigma\langle I\rangle$ where $\langle I\rangle$ is the mean of the intensity measurements, I_i, and the summation extends over all reflections.

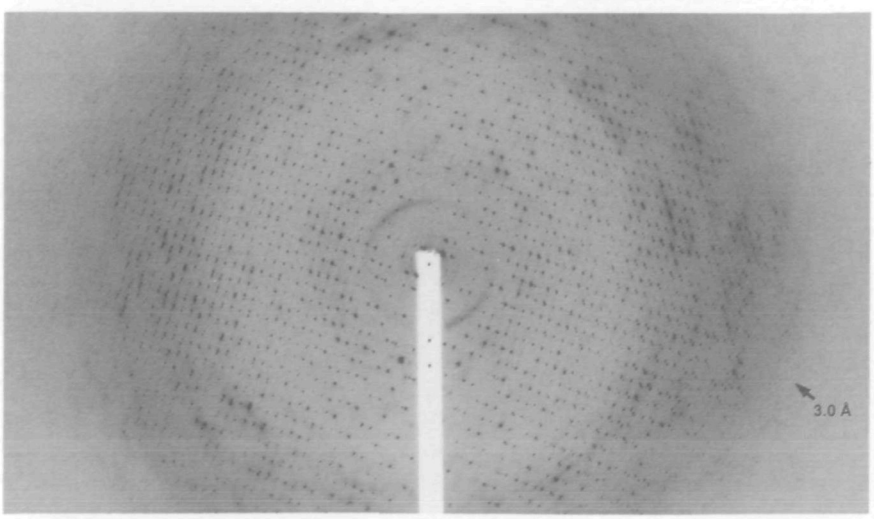

Fig. 4. **Oscillation photograph of *A. xylanus* AhpC crystals taken with synchrotron radiation.** The oscillation range is 6.1° and the crystal-to-film distance is 430 mm.

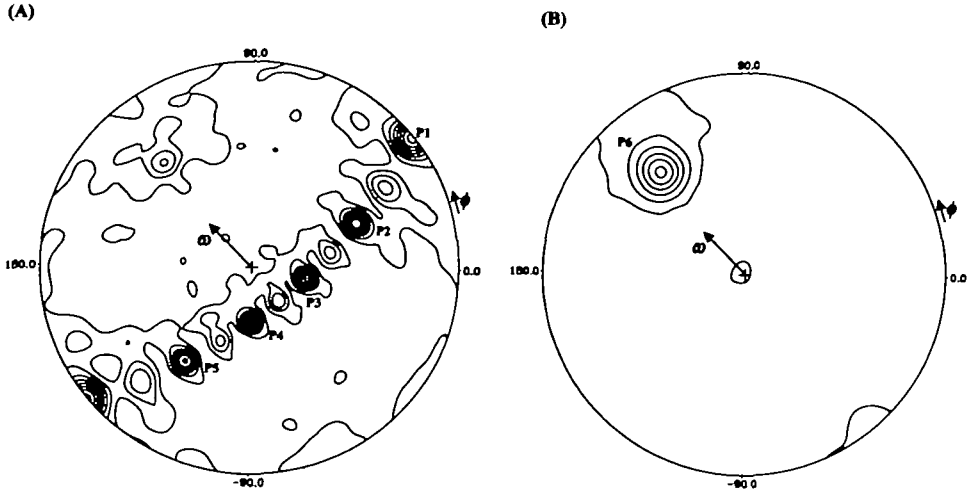

Fig. 5. **Self-rotation function calculated for *A. xylanus* AhpC data set at 293 K.** (A) Section $\kappa = 180^\circ$ ($= 360^\circ/2$) and (B) 72° ($= 360^\circ/5$). The orientation of the rotation axis κ is defined by ω (angle from z axis) and ϕ (angle in the x, y plane) with respect to the orthogonalized axes. The stereographic projections of each κ section are shown with ω and ϕ as the radial and angular coordinates, respectively. Contour lines are drawn starting at 10% in 10% increments. Observed highest peaks (P1-P6) are listed in Table II.

TABLE II. **Highest peaks in self-rotation function of the *A. xylanus* AhpC crystal.**

Peak	ω (°)	ϕ (°)	κ (°)	Peak height (%)
P1	89.5	40.0	180.0	84.4
P4	29.3	269.9	180.0	81.9
P7	66.8	130.3	144.0	73.5
P3	28.7	348.9	180.0	71.3
P2	57.0	23.9	180.0	68.7
P6	66.6	130.1	72.0	62.9
P5	57.8	236.0	180.0	61.8

ω, ϕ, κ are the polar angles in the orthogonal frame with the Brookhaven format. Origin peak ($\omega = 0$, $\phi = 0$, $\kappa = 0$) was set to 100%.

and 72° (in Polar angles) sections reveal the twofold and fivefold molecular symmetry orientations, respectively (Fig. 5), and the observed highest peaks are listed in Table II.

Peroxidase Activity Assay of A. xylanus NADH Oxidase-AhpC System—Turnover studies of H_2O_2 reductase activities were carried out to investigate the dependence of the *A. xylanus* NADH oxidase-AhpC system on ionic strength. *A. xylanus* AhpC and NADH oxidase mixtures were prepared in 100 mM HEPES-NaOH buffer (pH 7.5) containing salt at each concentration. The reaction was started under aerobic conditions at 25°C by mixing 700 μl of protein solution with 50 μl of substrate mixtures containing H_2O_2 and NADH. The final concentrations of *A. xylanus* AhpC, NADH oxidase, H_2O_2, and NADH after mixing were set to 144, 0.02, 500, and 150 μM, respectively. The reaction was monitored at 340 nm in a temperature controlled spectrophotometer (U-3300, Hitachi, Tokyo) (Fig. 6).

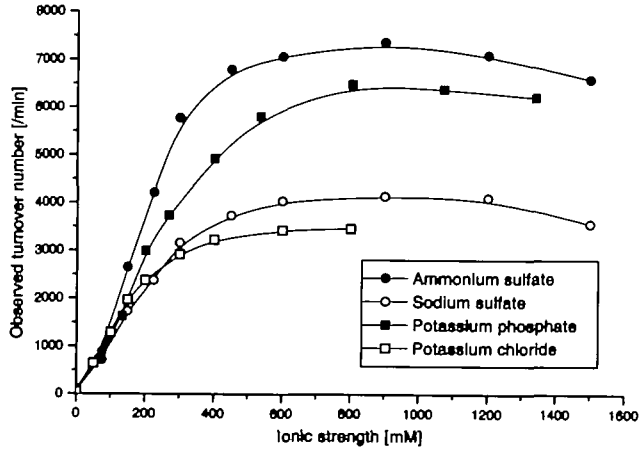

Fig. 6. **Peroxidase activities of the *A. xylanus* NADH oxidase-AhpC system *versus* ionic strength.** Activity assays were performed at 25°C with various salts: ammonium sulfate (○), sodium sulfate (●), potassium phosphate (□), and potassium chloride (■).

RESULTS AND DISCUSSION

Characterization of the Oligomeric State of A. xylanus AhpC—A highly homogeneous single peak of *A. xylanus* AhpC was observed following gel-filtration column chromatography in the presence of 100 mM sodium sulfate (Fig. 1). The molecular mass of this peak, determined from a plot of the logarithm of molecular weight *versus* mobility (data not shown), corresponds to approximately 200-220 kDa. The DLS assays gave a similar molecular mass in the presence of 100 mM sodium sulfate (Fig. 2, the effect of ionic strength is discussed in the next section). These results suggest that *A. xylanus* AhpC will oligomerize in solution to form a large homo-assembly composed of 5-6 dimers.

This oligomeric state of *A. xylanus* AhpC was confirmed by a preliminary X-ray crystallographic study, where the self-rotation function of the native crystal gives information about the molecular symmetry. As crystals were not obtained with salts containing chloride, phosphate or sulfate, the acetic anion might play a specific role in the crystallization process of *A. xylanus* AhpC. In X-ray experiments or *A. xylanus* AhpC crystals at 293 K, the diffraction spots were sharp and clean at 20-4 Å resolution, but tended to be broad and anisotropic at higher resolution (>4 Å), as shown in Fig. 4. Although the frozen crystals at 100 K were quite stable against synchrotron radiation damage, the mosaicity of the crystals became five times greater (>1.0°) with greater anisotropy than that observed in crystals at 293 K. Further optimization for the cryo conditions are necessary to apply this technique to determining the structure of *A. xylanus* AhpC at an atomic resolution.

A comparison of the self-rotation function, calculated for the diffraction data at 293 and 100 K, revealed the same molecular symmetry for *A. xylanus* AhpC. Five non-crystallographic twofold axes were identified at $\kappa = 180°$ by strong peaks on a single plane in the self-rotation map (Fig. 5A). Fivefold axes were also identified at $\kappa = 72°$ (Fig. 5B) and 144°, perpendicularly to the five twofold axes. As the space group of this crystal is *P*1, all these observed peaks correspond to the local molecular symmetry of *A. xylanus* AhpC assembly. Based on these results, a hypothetical assembly model with a decameric symmetry was constructed in the unit cell (Fig. 7). Assuming this model, the V_M values are calculated to be 3.0 Å³/Da (293 K) and 2.8 Å³/Da (100 K), which lie in the range of 1.8-3.5 Å³/Da that is usual for protein crystals (*31*). The present decameric model of *A. xylanus* AhpC obtained crystallographically is also consistent with the molecular mass determined by the gel-filtration column chromatography and DLS.

Effects of Ionic Strength on the Oligomerization of A. xylanus AhpC and the Peroxidase Activity of the NADH Oxidase-AhpC System—The DLS assays showed that the oligomeric state of *A. xylanus* AhpC is significantly affected by the ionic strength of the solution (Fig. 2). The results obtained with four different salts fall within the range of the experimental error, suggesting that the dominant factor influencing the oligomeric state is not the salt type but the ionic strength. The decamer of *A. xylanus* AhpC shown in Fig. 7 would exist in solution at ionic strengths higher than 300 mM. The protein solution tended to be more clearly mono-disperse at high ionic strength than at low ionic strength in DLS (data not shown), suggesting that *A. xylanus* AhpC molecules oligomerize uniformly as decamers at high ionic strength (>300 mM), but exist as a mixture of incomplete assembly states (dimer, tetramer, hexamer, *etc.*) at low ionic strength, as illustrated schematically in Fig. 9.

When the H_2O_2 reductase activity of the *A. xylanus* NADH oxidase-AhpC system was measured in the absence of salt (under low ionic strength), the activity was only 5% of that in the presence of 150 mM ammonium sulfate (ionic strength = 450 mM), even if the concentration of AhpC was extremely high (144 μM), as shown in Fig. 6. Further investigations showed that the peroxidase activity is remarkably dependent on ionic strength, similar to the previous results for *A. xylanus* NADH oxidase/*S. typhimurium* AhpC (*5*). The V_{max} and K_m values for *S. typhimurium* AhpC in the presence of 150 mM ammonium sulfate (168 s^{-1} and 13.5 mM, respectively) are similar in magnitude to those for *A. xylanus* AhpC (152 s^{-1} and 15.4 mM, respectively), indicating that both *A. xylanus* and *S. typhimurium* AhpC proteins are able to reduce H_2O_2 with *A. xylanus* NADH oxidase in the presence of 150 mM ammonium sulfate. The effect of salts on the basal activity of the *A. xylanus* NADH oxidase-AhpC system was expressed as a function of the total ionic strength (Fig. 6), where the activity was highest with ammonium sulfate and lowest with potassium chloride. This trend is quite similar to that found for enhancing hydrophobic interactions (*32*), suggesting that the stimulation of *A. xylanus* NADH oxidase-AhpC activity by salts might be due to an enhancement of the hydrophobic interactions between protein molecules (*5*). As the oligomeric state of *A. xylanus* AhpC does not depend on the salt type but on ionic strength, the differences observed with these four salts might be due to an enhancement of the hydrophobic interactions between the AhpC and NADH oxidase molecules rather than to effects causing homo-oligomerization.

Both the oligomerization of *A. xylanus* AhpC and the peroxidase activity of the NADH oxidase-AhpC system are significantly correlated with ionic strength for each salt (Figs. 2 and 6). Thus we can show the relationship between the peroxidase activity and molecular mass by eliminating the common parameter, ionic strength (Fig. 8). As the concentration of *A. xylanus* NADH oxidase in the activity assays was quite low (0.02 μM) compared with that of AhpC (144 μM, the same also in DLS), the effect of NADH oxidase on the oligomerization of AhpC might be negligible. The observed turnover number is saturated around a molecular mass of 200 kDa (Fig. 8), which corresponds to ten AhpC subunits. This shows that *A. xylanus* AhpC exists as a decamer when it is highly activated by the addition of

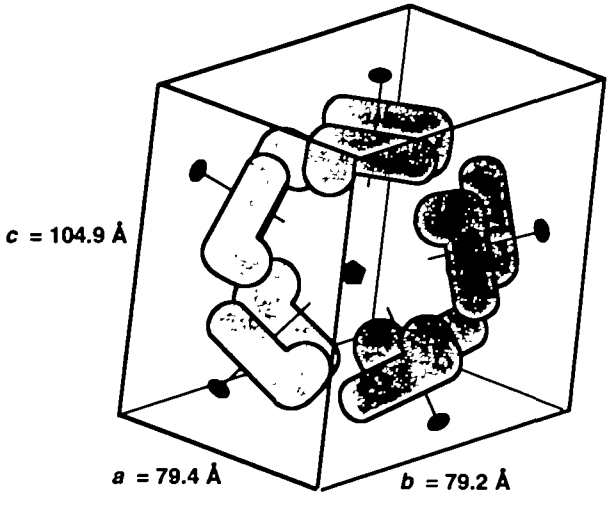

Fig. 7. **Packing model for *A. xylanus* AhpC in the unit cell of the *P*1 crystal.** The homodimers are related by a fivefold axis.

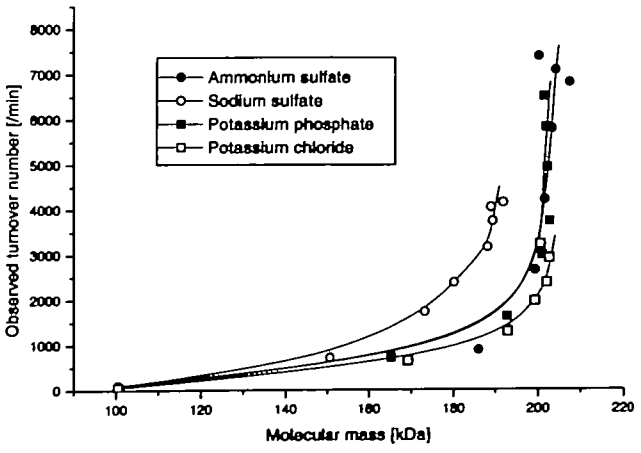

Fig. 8. **Peroxidase activity of the *A. xylanus* NADH oxidase-AhpC system and the oligomeric state of AhpC.** The correlation between activity and molecular mass was deduced from the DLS experiment (Fig. 2) and the peroxidase activity measurements (Fig. 6): ammonium sulfate (○), sodium sulfate (●), potassium phosphate (□), and potassium chloride (■).

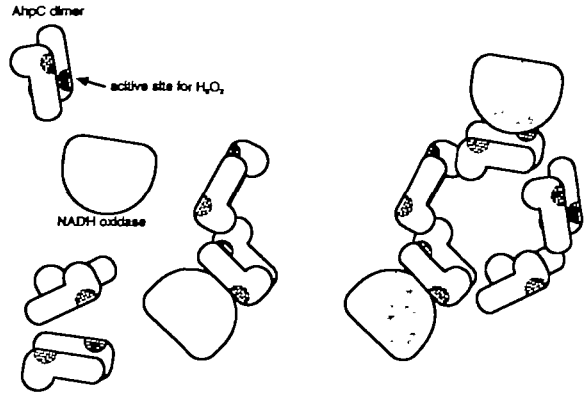

Fig. 9. **Hypothetical model showing the oligomeric nature of *A. xylanus* AhpC at high and low ionic strengths, with the effect on the peroxidase activity of the NADH oxidase-AhpC system.** (A) At low ionic strength with few hydrophobic interactions between AhpC dimers, most of AhpC exists as dimers and NADH oxidase interacts randomly with the dimer surfaces. (B) At high ionic strength, AhpC dimers can pentamerize due to the preferable hydrophobic interactions. The accessible surface of the AhpC molecules is reduced by oligomerization, and the active site of AhpC, which captures H_2O_2 molecules, is exposed to the solvent.

salts, and also suggests that the decamerization of AhpC might be required for the activation of the *A. xylanus* NADH oxidase-AhpC system.

This significant effect of oligomerization on the peroxidase activity can be explained in the following two ways. One possibility is that the decamerization of *A. xylanus* AhpC might induce small conformational changes around the active sites. The crystal structure of RuBisCO (ribulose-1,5-biphosphate carboxylase/oxygenase), a CO_2-fixing enzyme in the Calvin cycle, showed that the catalytic rate could be promoted by small conformational changes caused by oligomerization (*33, 34*). The decamerization of *A. xylanus* AhpC might enhance the selectivity for H_2O_2 in the same way, which would also be preferable for the interaction with NADH oxidase. The other possibility is that the reduction of the accessible surface of *A. xylanus* AhpC by oligomerization could be important. Coupled with the reduced accessible surface by decamerization, the active site of *A. xylanus* AhpC might be exposed to the solvent by the alignment of subunits (Fig. 9). This would suppress H_2O_2 and NADH oxidase molecules from interacting with surfaces other than the active sites of AhpC, and might enhance the turnover number of H_2O_2.

The molecules of human Prx, a 1-Cys AhpC, exist as homodimers in the crystal structure (*35*). The structure shows the catalytic Cys47 located at the bottom of a narrow pocket, which is considered to be significant for the selectivity for H_2O_2 molecules. On the other hand, no structure of a 2-Cys AhpC is yet available, mainly because of crystallization difficulties due to the heterogeneous intermolecular disulfide bonds. As the sequence homology between *A. xylanus* AhpC and human Prx is only 29%, the three-dimensional structure of a 2-Cys AhpC at the atomic level is indispensable to understand the systematic reaction mechanism of the NADH oxidase-AhpC system. The structure determination of the *A. xylanus* AhpC decamer *via* phase determination with MIR (multiple isomorphous replacement) is in progress. This should also show how the oligomerization of *A. xylanus* AhpC affects the H_2O_2 reduction mechanism of the *A. xylanus* NADH oxidase-AhpC system.

We are indebted to Drs. N. Sakabe, N. Watanabe, M. Suzuki, and N. Igarashi of the Photon Factory, Institute of Material Structure Science, High Energy Accelerator Research Organization, for their kind help in the X-ray diffraction work, which was performed under the approval of the Photon Factory Advisory Committee (Proposal No. 98G164). K.M. is a member of the Sakabe Project of TARA (Tsukuba Advanced Research Alliance), University of Tsukuba. Thanks are also due to S. Sasaki in the laboratory of Y. Niimura for protein purification.

REFERENCES

1. Sies, H. (1993) Strategies of antioxidant defense. *Eur. J. Biochem.* **215**, 213-219
2. Jacobson, F.S., Morgan, R.W., Christman, M.F., and Ames, B.N. (1989) An alkyl hydroperoxide reductase from *Salmonella typhimurium* involved in the defense of DNA against oxidative damage. *J. Biol. Chem.* **264**, 1488-1496
3. Chae, H.Z., Robison, K., Poole, L.B., Church, G., Storz, G., and Rhee, S.G. (1994) Cloning and sequencing of thiol-specific antioxidant from mammalian brain: alkyl hydroperoxide reductase and thiol-specific antioxidant define a large family of antioxidant enzymes. *Proc. Natl. Acad. Sci. USA* **91**, 7017-7021
4. Chae, H.Z., Uhm, T.B., and Rhee, S.G. (1994) Dimerization of thiol-specific antioxidant and the essential role of cysteine 47. *Proc. Natl. Acad. Sci. USA* **91**, 7022-7026
5. Niimura, Y., Poole, L.B., and Massey, V. (1995) *Amphibacillus xylanus* NADH oxidase and *Salmonella typhimurium* alkyl-hydroperoxide reductase flavoprotein components show extremely high scavenging activity for both alkyl hydroperoxide and hydrogen peroxide in the presence of *S. typhimurium* alkyl-hydroperoxide reductase 22-kDa protein component. *J. Biol. Chem.* **270**, 25645-25650
6. Chae, H.Z., Chung, S.J., and Rhee, S.G. (1994) Thioredoxin-dependent peroxide reductase from yeast. *J. Biol. Chem.* **269**, 27670-27678
7. Niimura, Y., Yanagida, F., Uchimura, T., Ohara, N., Suzuki, K., and Kozaki, M. (1987) A new facultative anaerobic xylan-digesting bacterium which lacks cytochrome, quinone, and catalase. *Agric. Biol. Chem.* **51**, 2271-2275
8. Koyama, N., Niimura, Y., and Kozaki, M. (1988) Bioenergetic properties of a facultatively anaerobic alkalophile. *FEMS Microbiol. Lett.* **49**, 123-126
9. Niimura, Y., Yanagida, F., Suzuki, K., Komagata, K., and Kozaki, M. (1990) *Amphibacillus xylanus* gen. nov., sp. nov., a facultatively anaerobic sporeforming xylan-digesting bacterium which lacks cytochrome, quinone, and catalase. *Int. J. Syst. Bacteriol.* **40**, 297-301
10. Niimura, Y., Koh, E., Uchimura, T., Ohara, N., and Kozaki, M. (1989) Aerobic and anaerobic metabolism in a facultative anaerobe EP01 lacking cytochrome, quinone and catalase. *FEMS Microbiol. Lett.* **61**, 79-84
11. Poole, L.B. and Ellis, H.R. (1996) Flavin-dependent alkyl hydroperoxide reductase from *Salmonella typhimurium*. 1. Purification and enzymatic activities of overexpressed AhpF and AhpC proteins. *Biochemistry* **35**, 56-64
12. Poole, L.B. (1996) Flavin-dependent alkyl hydroperoxide reductase from *Salmonella typhimurium*. 2. Cystine disulfides involved in catalysis of peroxide reduction. *Biochemistry* **35**, 65-75
13. Ellis, H.R. and Poole, L.B. (1997) Roles for the two cysteine residues of AhpC in catalysis of peroxide reduction by alkyl hydroperoxide reductase from *Salmonella typhimurium*. *Biochemistry* **36**, 13349-13356
14. Kim, K., Kim, I.H., Lee, K.Y., Rhee, S.G., and Stadtman, E.R. (1988) The isolation and purification of a specific "protector"

protein which inhibits enzyme inactivation by a thiol/Fe(III)/O_2 mixed-function oxidation system. *J. Biol. Chem.* **263**, 4704-4711
15. Cleland, J.L. and Wang, D.I. (1990) Refolding and aggregation of bovine carbonic anhydrase B: quasi-elastic light scattering analysis. *Biochemistry* **29**, 11072-11078
16. Gast, K., Damaschun, G., Misselwitz, R., and Zirwer, D. (1992) Application of dynamic light scattering to studies of protein folding kinetics. *Eur. Biophys. J.* **21**, 357-362
17. Georgalis, Y., Umbach, P., Raptis, J., and Saenger, W. (1997) Lysozyme aggregation studied by light scattering. I, II. *Acta Crystallogr.* **D53**, 691-702; 703-712
18. Kuehner, D.E., Heyer, C., Rämsch, C., Fornefeld, U.M., Blanch, H.W., and Prausnitz, J.M. (1997) Interactions of lysozyme in concentrated electrolyte solutions from dynamic light-scattering measurements. *Biophys. J.* **73**, 3211-3224
19. Czurylo, E.A., Hellweg, T., Eimer, W., and Dabrowska, R. (1997) The size and shape of caldesmon and its fragments in solution studied by dynamic light scattering and hydrodynamic model calculations. *Biophys. J.* **72**, 835-842
20. Kam, Z., Shore, H.B., and Feher, G. (1978) On the crystallization of proteins. *J. Mol. Biol.* **123**, 539-555
21. Thibault, F., Langowski, J., and Leberman, R. (1992) Pre-nucleation crystallization studies on aminoacyl-tRNA synthetases by dynamic light-scattering. *J. Mol. Biol.* **225**, 185-191
22. Skouri, M., Munch, J.P., Lorber, B., Giegé, R., and Candau, S. (1992) Interactions between lysozyme molecules under precrystallization conditions studied by light scattering. *J. Crystal Growth* **122**, 14-20
23. Zulauf, M. and D'Arcy, A. (1992) Light scattering of proteins as a criterion for crystallization. *J. Crystal Growth* **122**, 102-106
24. Mikol, V., Hirsch, E., and Giegé, R. (1990) Diagnostic of precipitant for biomacromolecule crystallization by quasi-elastic light-scattering. *J. Mol. Biol.* **213**, 187-195
25. D'Arcy, A. (1994) Crystallizing proteins—A rational approach? *Acta Crystallogr.* **D50**, 469-471
26. Ferré-D'Amaré, A.R. and Burley, S.K. (1994) Use of dynamic light scattering to assess crystallizability of macromolecules and macromolecular assemblies. *Structure* **2**, 357-359
27. McPherson, A. (1982) *Preparation and Analysis of Protein Crystals,* pp. 94-96, Krieger, Malabar, FL
28. Sakabe, N., Ikemizu, S., Sakabe, K., Higashi, T., Nakagawa, A., Watanabe, N., Adachi, S., and Sasaki, K. (1995) Weissenberg camera for macromolecules with imaging plate data collection system at Photon Factory: Present status and future plan. *Rev. Sci. Instrum.* **66**, 1276-1281
29. Otwinowski, Z. and Minor, W. (1997) Processing of X-ray diffraction data collected in oscillation mode. *Methods Enzymol.* **276**, 307-326
30. Rossman, M.G. and Blow, D.M. (1962) The detection of sub-units within the crystallographic asymmetric unit. *Acta Crystallogr.* **15**, 24-31
31. Matthews, B.W. (1968) Solvent content of protein crystals. *J. Mol. Biol.* **33**, 491-497
32. Englard, S. and Seifter, S. (1990) Precipitation techniques. *Methods Enzymol.* **182**, 285-300
33. Hartman, F.C. and Harpel, M.R. (1994) Structure, function, regulation, and assembly of D-ribulose-1,5-bisphosphate carboxylase/oxygenase. *Annu. Rev. Biochem.* **63**, 197-234
34. Schneider, G., Knight, S., Andersson, I., Brändén, C.I., Lindqvist, Y., and Lundqvist, T. (1990) Comparison of the crystal structures of L_2 and L_8S_8 Rubisco suggests a functional role for the small subunit. *EMBO J.* **9**, 2045-2050
35. Choi, H.J., Kang, S.W., Yang, C.H., Rhee, S.G., and Ryu, S.E. (1998) Crystal structure of a novel human peroxidase enzyme at 2.0 Å resolution. *Nat. Struct. Biol.* **5**, 400-406